Complete transformation of ZnO and CuO nanoparticles in culture medium and lymphocyte cells during toxicity testing

Journal:	*Nanotoxicology*
Manuscript ID	TNAN-2016-0291.R1
Manuscript Type:	Short Communication
Date Submitted by the Author:	n/a
Complete List of Authors:	Ivask, Angela; University of South Australia, Future Industries Institute Scheckel, Kirk; National Risk Management Research Laboratory Kapruwan, Pankaj; University of South Australia, Future Industries Institute Stone, Vicki; Heriot-Watt University, School of Life Sciences Yin, Hong; CSIRO Manufacturing Flagship Volecker, Nicolas; University of South Australia, Future Industries Institute Lombi, Enzo; University of South Australia, Future Industries Institute
Keywords:	copper oxide, zinc oxide, speciation, mammalian cells
Abstract:	Here we present evidence on complete transformation of ZnO and CuO nanoparticles, which are among the most heavily studied metal oxide particles, during 24 h in vitro toxicological testing with human T-lymphocytes. Synchrotron radiation-based X-ray absorption near edge structure (XANES) spectroscopy results revealed that Zn speciation profiles of 30 nm and 80 nm ZnO nanoparticles, and ZnSO4 exposed cells were almost identical with the prevailing species being Zn-cysteine. This suggests that ZnO nanoparticles are rapidly transformed during a standard in vitro toxicological assay, and are sequestered intracellularly, analogously to soluble Zn. Complete transformation of ZnO in the test conditions was further supported by almost identical Zn spectra in medium to which ZnO nanoparticles or ZnSO4 was added. Likewise, Cu XANES spectra for CuO and CuSO4 –exposed cells and cell culture media were similar. These results together with our observation on similar toxicological profiles of ZnO and soluble Zn, and CuO and soluble Cu, underline the importance of

	dissolution and subsequent transformation of ZnO and CuO nanoparticles during toxicological testing and provide evidence that the nano-specific effect of ZnO and CuO nanoparticulates is negligible in this system. We strongly suggest to account for this aspect when interpreting the toxicological results of ZnO and CuO nanoparticles.

Complete transformation of ZnO and CuO nanoparticles in culture medium and lymphocyte cells during toxicity testing

Angela Ivask†‖, Kirk G. Scheckel‡, Pankaj Kapruwan†, Vicki Stone|, Hong Yin#, Nicolas H. Voelcker†, Enzo Lombi†*

† Future Industries Institute, University of South Australia, Mawson Lakes, SA, Australia

‡ National Risk Management Research Laboratory, US Environmental Protection Agency, USA

| Heriot-Watt University, Edinburgh, United Kingdom

CSIRO Manufacturing, Clayton, VIC 3168, Australia

‖ Current address: Laboratory of Environmental Toxicology, National Institute of Chemical Physics and Biophysics, Tallinn, Estonia

* Corresponding author: Future Industries Institute, University of South Australia, Mawson Lakes, 5095 SA, Australia. Phone: +61883026267, Email: Enzo.Lombi@unisa.du.au

Abstract

Here we present evidence on complete transformation of ZnO and CuO nanoparticles, which are among the most heavily studied metal oxide particles, during 24 h *in vitro* toxicological testing with human T-lymphocytes. Synchrotron radiation-based X-ray absorption near edge structure (XANES) spectroscopy results revealed that Zn speciation profiles of 30 nm and 80 nm ZnO nanoparticles, and $ZnSO_4$ exposed cells were almost identical with the prevailing species being Zn-cysteine. This suggests that ZnO nanoparticles are rapidly transformed during a standard *in vitro* toxicological assay, and are sequestered intracellularly, analogously to soluble Zn. Complete transformation of ZnO in the test conditions was further supported by almost identical Zn spectra in medium to which ZnO nanoparticles or $ZnSO_4$ was added. Likewise, Cu XANES spectra for CuO and $CuSO_4$ –exposed cells and cell culture media were similar. These results together with our observation on similar toxicological profiles of ZnO and soluble Zn, and CuO and soluble Cu, underline the importance of dissolution and subsequent transformation of ZnO and CuO nanoparticles during toxicological testing and provide evidence that the nano-specific effect of ZnO and CuO nanoparticulates is negligible in this system. We strongly suggest to account for this aspect when interpreting the toxicological results of ZnO and CuO nanoparticles.

Keywords: copper oxide, zinc oxide, nanoparticles, speciation, mammalian cells

Background

Although a number of studies have discussed the transformation of nanoparticles during toxicity testing, the extent and nature of these transformations is relatively difficult to qualitatively assess let alone to quantify. In the case of metal oxides, one of the major transformations could be particle dissolution which has been demonstrated for Zn, Cu and Ag-containing nanoparticles (see reviews by Ivask et al. (2012) and Zhang et al. (2015)). One of the main methods that has been used to study the dissolution of nanoparticles during toxicological testing has been separation of nanoparticulates and dissolved ions by centrifugation or membrane filtration. For example, using centrifugation, the dissolution of CuO in cell culture medium has been shown to reach 40% (Karlsson et al., 2014; Semisch et al., 2014; Ivask et al., 2015) and the dissolution of ZnO 50% (Turney et al., 2012). However, there is strong evidence that nanoparticles dissolution determined by different methodologies may significantly vary. Turney et al. (2012) showed that dissolution of ZnO nanoparticles was 5-fold different depending whether centrifugation or a dialysis membrane was used to separate particles and ions. Moreover, dissolution studies are often difficult to translate to real experimental conditions (e.g., in the presence of cells) and they do not provide information on localized (e.g., intracellular) dissolution or other transformations that may take place with nanoparticles during the test.

One alternative method to assess nanoparticle transformation and speciation during toxicological testing is synchrotron radiation-based X-ray absorption near edge structure (XANES) spectroscopy. XANES is capable of providing relative quantitative information about elemental speciation without prior separation of particulates and ions (Qu et al., 2011, Gräfe et al., 2014). This method is being increasingly deployed in the field of nanotoxicology (Gilbert et al., 2012; Jiang et al., 2015; Wang et al., 2015) due to recent enabling advances.

The aim of this study was to reveal the speciation of nanoparticulate ZnO and CuO before and during toxicological testing. Even though the number of publications on ZnO and CuO nanoparticles and their toxicity is significant, information on dissolution and transformation of those particles in the test conditions is usually insufficient and thus judgement on which factors are driving their toxic effects is difficult. In this study, we used synchrotron radiation-based XANES and resulting K-edge Zn and Cu spectra to assess the speciation of 30 and 80 nm ZnO nanoparticles and 15 nm CuO nanoparticles in human T-lymphocyte cells and in their exposure medium over a 24 h time frame which is standard for *in vitro* toxicological assays. The results indicated prompt transformation of the nanoparticles in the test medium. Furthermore, speciation profiles of ZnO and CuO inside the cells overlapped with soluble Zn and Cu, respectively, suggesting that cellular transformation and

sequestration of nanoparticles and their ionic counterparts were similar. This finding is significant for interpretation of past and future toxicological results of ZnO and CuO nanoparticles.

Materials and Methods

Nanoparticles

Zinc oxide nanoparticles, 31.8±8.9 nm in diameter (surface area 27.4 m^2/g, ζ potential 14.2 mV, further referred to as ZnO-30) and 89.7±24.0 nm in diameter (surface area 4.6 m^2/g, ζ potential 20.0 mV further referred to as ZnO-80) were synthesized as in Yin et al. (2010). CuO nanoparticles, crystalline and 15-20 nm in diameter, were from Plasma Chem, GmbH, Berlin, Germany. Detailed characterization of these nanoparticles was published earlier (Gosens et al., 2015). TEM images of the particles (Figure 1) were taken using a transmission electron microscope (TEM, JEOL JEM2100F) at 200 kV. For that, 10 µL of nanoparticle suspension (50 µg/mL) was pipetted onto 300 mesh Cu grids covered by carbon film (ProSciTech). Particles were allowed to settle on the grids for 5 min and excess liquid was removed with a paper towel; the grids were then dried overnight before imaging. Primary diameter of the particles (average for 20-30 particles) was measured using Gatan software. Hydrodynamic diameter (Dh) of the nanoparticles dispersions (≈10 µg/mL, vortexed in water or cell culture medium and sonicated in a water bath (Branson) for 2-3 min) in water and in cell culture medium (RPMI medium with 10% FBS and other supplements as described below) was measured using dynamic light scattering (DLS) with a PSS Nicomp 380 particle sizer using number-based size distribution.

Cytotoxicity assay

Human T-lymphocyte cell line Jurkat (Clone E6-1, ATCC® TIB-152™) was chosen because of its relevance in nanoparticle toxicity and non-adherent nature which facilitated harvesting and preparation of the cells for synchrotron analysis. The cells were maintained in RPMI 1640 medium containing 4.5 g glucose/L, 1mM Na-pyruvate, 2 mM L-glutamine, 100 U/mL penicillin, 100 µg/mL streptomycin and 10% FBS. For routine culturing, the cell density was maintained between $2*10^5$ and $2*10^6$ cells/mL. For cytotoxicity experiments $5*10^5$ cells were used. A volume of 100 µL of cell suspension was pipetted onto 96-well plates and 100 µL of ZnO and CuO nanoparticle suspensions or solution of $ZnSO_4$ (Labserv) and $CuSO_4$ (Merck) ranging from 0.3 to 300 µg/mL in cell culture medium was added; after that, the plates were incubated at 37 °C and 5% CO_2 for 24 h. Each concentration of nanoparticles was analyzed in three replicates and the resazurin assay that was used to evaluate cell viability was repeated on three different days. For the assay, resazurin at 30 µg/mL was added to each well and plates were incubated for 4 h at 37 °C, 5% CO_2. Resazurin reduction due to cell metabolic activity was measured with a fluorescence plate reader (Synergy, Biotek) using excitation/emission filters 530/590 nm. For background control, resazurin was added also to wells with cell culture medium (no cells). These background values were subtracted from cell readings

before calculations. The cytotoxicity assay was performed in at least three independent experiments. Percentages of viable cells in Cu and Zn treatments compared to non-exposed cells were calculated; half (50%) effective concentration (EC_{50}), 20% (EC_{20}), 10% (EC_{10}) and 5% (EC_5) effective concentrations with 95% confidence intervals and standard error (SE) in µg Cu or Zn/mL were calculated using Prism software (GraphPad). Statistical differences between EC_{50}, EC_{20}, EC_{10} and EC_5 of CuO and $CuSO_4$ and of ZnO particles and $ZnSO_4$ were analyzed using one-way ANOVA in MS Excel.

Collection and analysis of XANES spectra

For Zn and Cu speciation analysis by XANES, the cells were exposed to CuO and ZnO nanoparticles, and $CuSO_4$ and $ZnSO_4$ as controls for dissolved Zn^{2+} and Cu^{2+}. For synchrotron experiments, non-toxic concentrations that affected only 5% cells in 24 h cytotoxicity assay, were selected. A volume of 70 mL of medium containing $5*10^5$ Jurkat cells was exposed for 24 h at 37 °C and 5% CO_2 to 2 µg Cu/mL of CuO and $CuSO_4$, and 3 µg Zn/mL of ZnO-30, ZnO-80 nanoparticles and $ZnSO_4$. Exposed cells were centrifuged at 200 g for 5 min and washed two times with PBS buffer. The cell pellet (≈100 mg from each exposure condition) was then concentrated in a microcentrifuge tube and dried overnight in a freeze-dryer (Modulyod, Thermo Electron Corp.). Non-exposed cells were prepared for comparison. To analyse the speciation of Zn and Cu in cell culture medium, 100 mL of cell culture medium was spiked with 2 µg Cu/mL of CuO nanoparticles and $CuSO_4$, and 3 µg Zn/mL of ZnO-30, ZnO-80 nanoparticles and $ZnSO_4$, and incubated for 24 h at 37 °C and 5% CO_2. After incubation, the cell culture medium was freeze-dried; non-spiked cell culture medium was used as a control. Between 2 and 5 mg of dried cells or cell culture medium were mounted using polymide (Kapton) tape onto a sample holder for XANES analysis, which was conducted at Sector 10-BM, Advanced Photon Source, Argonne, USA (Kropf et al., 2010). The storage ring operated at 7 GeV in top-up mode. A liquid N_2cooled double crystal Si(111) monochromator was used to select the incident photo energies and a platinum-coated mirror was used for harmonic rejection. Calibration was performed by assigning the first derivative inflection point of the K-edge of Cu (8979 eV) or Zn (9659 eV) metal foils with simultaneous collection of the reference for each scan for calibration of sample spectra. XANES spectra were collected in triplicate in transmission and fluorescence using a 4-element Vortex fluorescence detector.

Collected Zn and Cu K-edge XANES spectra were analyzed using XAS data and analysis software Athena (Ravel and Newville, 2005). Data analysis involved energy calibration, background subtraction and normalization. Spectra of each sample were subjected to principal component analysis that revealed that four components were explaining >99% of the variability in the samples.

Thus, linear combination fitting (LCF) of each sample (from−20 eV below to +80eV above the edge) was done using XANES spectra of standard Zn or Cu compounds and up to four combinations. For Zn samples, ZnO nanoparticles, Zn-cysteine complex, Zn-phosphate complex, Zn-citric acid and Zn-acetic acid complex were used as standard spectra. For Cu samples, CuO nanoparticles, Cu-histidine complex, Cu-cysteine complex, Cu-citric acid complex or $Cu(OH)_2$ were used as standard spectra. The combination of standards that resulted in the best fit was chosen as the most likely representation of the sample.

Results and Discussion

In this study, we analyzed the cytotoxicity and speciation of Cu and Zn in media and cells exposed to soluble Cu and Zn salts, ≈15 nm CuO nanoparticles and ≈30 (ZnO-30) and 80 nm (ZnO-80) ZnO nanoparticles. In water and cell culture medium, the particles aggregated but remained relatively monodisperse (Figure 1). The hydrodynamic diameter of CuO nanoparticles and ZnO-30 in water and cell culture medium remained less than 100 nm. For ZnO-80, the hydrodynamic diameter was ≈125 nm in water and ≈195 nm in cell culture medium.

Results from cytotoxicity assessment of CuO and ZnO nanoparticles to human lymphocyte cells are shown on Figure 2. Overall, the EC_{50} concentrations for CuO and ZnO particles were in agreement with previous literature reporting EC_{50} values for ZnO and CuO nanoparticles between ≈5 and ≈100 µg Zn or Cu/mL (Bondarenko et al., 2013).

A large number of studies have suggested that the cytotoxicity of ZnO and CuO nanoparticles is driven by their dissolution and subsequent release of dissolved Zn and Cu (review by Ivask et al. (2014)). Therefore, we compared the cytotoxicities of ZnO and CuO with those of soluble forms of Zn and Cu ($ZnSO_4$ and $CuSO_4$, respectively; Figure 2). The results revealed that the EC_{50} values of the metal oxides and soluble forms of those metals were very similar when concentrations were expressed to represent the amount of metal ion in each treatment (Figure 2). This suggests that indeed, soluble Zn and Cu may drive the toxicity of all the Zn and Cu formulations. There were just small differences in cellular toxicities of oxide and soluble forms of Zn and Cu: CuO showed lower EC values than $CuSO_4$, while $ZnSO_4$ exhibited slightly higher toxicity than ZnO nanoparticles; and ZnO-80 was slightly less toxic than ZnO-30. None of the EC values of oxide and soluble forms of Cu and Zn were significantly different from each other, except for the CuO nanoparticles and $CuSO_4$ at the EC_5 and EC_{10} concentrations (Figure 2). Higher toxicity of CuO particles compared to soluble Cu which has also been shown in earlier studies (Karlsson et al., 2008; Shi et al., 2011; Ivask et al., 2015) can be

attributed to a "Trojan horse" effect which may facilitate the entry of Cu into the cells in nanoparticulate form (Cronholm et al., 2013).

Although our results of similar toxicities of ZnO and $ZnSO_4$, and CuO and $CuSO_4$ support the hypothesis of dissolution-driven cytotoxicity of ZnO and CuO, more evidence is required to strengthen this suggestion. In this study, we used synchrotron radiation-based XANES, a technique that enables sensitive assessment and relative quantification of nanoparticles speciation (Wang et al., 2013), to assess the transformation of ZnO and CuO particles in cells. To our knowledge, only one study on intracellular transformation of ZnO nanoparticles using synchrotron-based μ-XANES method has been published so far (Gilbert et al., 2012) and no such studies have been conducted on CuO nanoparticles. In addition to assessing particles speciation in cells, we also analysed the speciation of soluble Cu and Zn species in cells as well as Zn and Cu species present in non-exposed cells. Speciation of Cu and Zn in non-spiked cell culture medium, in CuO, ZnO, soluble Cu and Zn-spiked medium was also determined. Zinc and copper species in the samples were analyzed using linear combination fitting with selected Zn and Cu standard compounds which resulted in excellent fits for our samples (Figures 3 and 4 A-C). Analysis of Zn speciation in 24 h ZnO-30 and ZnO-80 exposed T-lymphocyte cells (Figure 3 D) showed that Zn-cysteine like complexes (30-60% of the total Zn) and Zn-phosphate (31-50%) were the prevailing Zn species with a relatively low fraction of ZnO (≈10% of total Zn in all the samples) and Zn acetate (3.5-13%) present. At this stage, we are unable to state in which cellular compartments the different Zn species were localized and whether Zn-cysteine and Zn-phosphate were present intracellularly as fine or nanoparticles. Further studies utilizing high resolution imaging capabilities (e.g., TEM) may provide answers to those questions. The high level of Zn-cysteine in ZnO-exposed cells is not surprising as cysteine is an amino acid with highest affinity to Zn (II) ions (Trzaskowski et al., 2008). Zinc speciation in ZnO-exposed cells was similar to that in non-exposed cells and in cells that were exposed to soluble Zn ($ZnSO_4$). It is interesting to note that in non-exposed cells and in those exposed to $ZnSO_4$, a small fraction of ZnO also showed up. We suggest that this was because of the presence of currently unknown Zn species with XANES spectral features overlapping with the XANES spectrum of ZnO. The result showing high degree in similarity in ZnO, soluble Zn and non-exposed cells ~~This result~~ indicates that ZnO particles undergo fast conversion in cell culture medium followed by cell-mediated transformations that are similar to those occurring with soluble Zn (including Zn that is already present in cell culture medium). The notion that ZnO is completely transformed during the testing period is supported by our data on ZnO speciation in cell culture medium (Figure 3 D). In accordance with the above results in the presence of cells, a similar Zn speciation was observed in cell culture medium in the absence of cells irrespective of whether the medium had only a basal concentration of Zn or was spiked with

a Zn formulation (to the EC_5 level) or which Zn formulation was used for spiking (ZnO-30, ZnO-80 or $ZnSO_4$). However, in contrast to the medium containing cells where Zn-cysteine was the prevailing species, in the absence of cells, most of the Zn in cell culture medium was in the form of Zn-phosphate and Zn-citrate. An intriguing finding is the presence of ZnO in cells and cell culture medium that had not been exposed to ZnO (Figure 3). We suggest that this was due to overlapping spectra of Zn standards and resulting misattribution during the fitting, or due to the formation of ZnO from Zn in non-spiked or $ZnSO_4$-spiked cell culture medium and cell suspension.

Analogously to ZnO, the Cu speciation results for cells and cell culture medium suggested total transformation of CuO particles (Figure 4). As seen from Figure 4 D, the XANES spectra of cells incubated with CuO and with soluble Cu were very similar and the same applied to cell culture medium that was spiked with CuO or soluble Cu (in the absence of cells). As for Cu, the prevailing species in CuO and soluble Cu exposed cells was Cu-cysteine (55-58%). Also, a small fraction of Cu-histidine (11-20%), Cu-citrate (4-11%) and CuO (15-22%) was identified. Again surprisingly, CuO was identified also in cells to which no nanoparticles were added ($CuSO_4$-exposed cells) and the fraction of CuO was even higher in $CuSO_4$-exposed cells than in CuO-exposed ones. This may suggest either the formation of CuO in Cu^{++}-cell mixture or interferences between XANES spectra of the different Cu species. In CuO and soluble Cu-spiked cell culture medium, we identified similar amounts of Cu-cysteine, Cu-histidine, Cu-citrate and CuO. Unfortunately, the Cu concentration in non-exposed cells and cell culture medium was too low to be detected with XANES (according to the manufacturer, 0.05-0.1 µg/mL Cu is present in cell culture medium whereas the detection limit for XANES is approximately 0.1 µg/mL in pure systems without interference from other fluorescing elements, i.e. Fe or Mn) and Cu speciation could not be calculated.

Conclusions

This study showed complete transformation of nanoparticulate CuO and ZnO at 2 µg/mL and 3 µg/mL, respectively, in conditions traditionally used for *in vitro* toxicological testing (24 h exposure in 10% FBS-containing cell culture medium at 37 °C and 5% CO_2). The transformation profiles of ZnO nanoparticles with different particle sizes (30 and 80 nm) and CuO nanoparticles were similar to those of $ZnSO_4$ and $CuSO_4$, respectively indicating that the metal oxide nanoparticles are completely transformed to the same species as their soluble counterparts. Therefore, the results of this study underline the importance of dissolution and subsequent transformation of nanosize ZnO and CuO during toxicological testing and demonstrate that the effect of nanoparticulates in the final

toxicological outcomes is negligible. As a result, we strongly suggest to account for dissolution and transformation when interpreting the toxicological results of ZnO and CuO nanoparticles.

Acknowledgements

Financial support from SA Government PRIF program project 'International Cluster on Nanosafety' and SUN project Funded by the European Commission (Grant agreement no. 604305) are kindly acknowledged. N.H.V. holds an Alexander von Humboldt Fellowship for Experienced Researchers. A.I is currently funded by Estonian Research Council grants PUT748 and SA Archimedes EQUiTANT. Although EPA contributed to this article, the views, interpretations, and conclusions expressed in this article are solely those of the authors and do not necessarily reflect or represent EPA's views or policies. This research used resources of the Department of Energy and the MRCAT member institutions, Advanced Photon Source, a U.S. Department of Energy (DOE) Office of Science User Facility operated for the DOE Office of Science by Argonne National Laboratory under Contract No. DE-AC02-06CH11357.

Figure captions

Figure 1. TEM images and hydrodynamic size of ZnO and CuO nanoparticles. (A-C) TEM images; primary particle size with standard deviation (based on 20-30 particles) is shown. (A) ZnO-30, (B) ZnO-80, (C) CuO. (D-E) hydrodynamic size (Dh) distribution of particles in water and in cell culture medium that was used in the cellular assays; average and standard deviation of Dh is shown on each graph. (D) ZnO-30, (E) ZnO-80, (F) CuO.

Figure 2. Cytotoxicity of different Zn and Cu formulations. Toxicity of ZnO-30, Zn0-80, $ZnSO_4$, CuO and $CuSO_4$ to T-lymphocyte cells in resazurin reduction assay after 24 h incubation. Black arrows indicate concentrations (ZnO-30, Zn0-80, $ZnSO_4$ at 3 µg Zn/mL, and CuO and $CuSO_4$ at 2 µg Cu/mL) that were selected for synchrotron experiments shown in Figures 3 and 4. Average half (50%) effective, 20, 10 and 5% effective concentrations ($EC_{50,}$ EC_{20}, EC_{10} and EC_5) with standard errors (SE) are shown under the graphs. * indicates significant ($p<0.05$) differences between CuO and $CuSO_4$.

Figure 3. Transformation of ZnO nanoparticles in T-lymphocyte cells and cell culture medium over 24 h. Speciation of ZnO nanoparticles and $ZnSO_4$ (added at 3 µg Zn/mL) in cell culture medium (A) and in cells (B). In (A-B) measured energy spectra (open symbols) and linear combination fit (red line) for standards (ZnO, Zn-citrate, Zn-acetate, Zn-cysteine, Zn-phosphate) is shown. (C) XANES spectra of Zn standards. (D) Linear combination fit-derived Zn speciation in ZnO-30, ZnO-80 and $ZnSO_4$-exposed cells and cell culture medium.

Figure 4. Transformation of CuO nanoparticles in T-lymphocyte cells and cell culture medium during 24 h. Speciation of CuO nanoparticles and $CuSO_4$ (added at 2 µg Cu/mL) in cell culture medium (A) and cells (B). In (A-B) measured energy spectra (open symbols) and linear combination fit (red line) for standards (CuO, Cu-citrate, Cu-histidine and Cu-cysteine) is shown. (C) XANES spectra of Cu standards. (D) Linear combination fitting-derived Cu speciation in CuO and $CuSO_4$-exposed cells and cell culture medium. <LOD – concentration below limit of detection.

References

Bondarenko O, Juganson K, Ivask A, Kasemets K, Mortimer M, Kahru A. 2013. Toxicity of Ag, CuO and ZnO nanoparticles to selected environmentally relevant test organisms and mammalian cells *in vitro*: a critical review. Arch Toxicol 87(7): 1181-1200.

Cronholm P, Karlsson HL, Hedberg J, Lowe TA, Winnberg L, Elihn K, Wallinder IO, Möller L. 2013. Intracellular uptake and toxicity of Ag and CuO nanoparticles: a comparison between nanoparticles and their corresponding metal ions. Small 9(7): 970-982.

Gilbert B, Fakra SC, Xia T, Pokhrel S, Mädler L, Nel AE. 2012. The fate of ZnO nanoparticles administered to human bronchial epithelial cells. ACS Nano 6(6): 4921-4930.

Gosens I, Kermanizadeh A, Jacobsen NR, Lenz A-G, Bokkers B, de Jong WH, Krystek P, Tran L, Stone V, Wallin H, Stoeger T, Cassee FR. 2015. Comparative hazard identification by a single dose lung exposure of zinc oxide and silver nanomaterials in mice. PLoS ONE 10(5): e0126934.

Gräfe M, Donner E, Collins RN, Lombi E. 2014. Speciation of metal(loid)s in environmental samples by X-ray absorption spectroscopy: A critical review. Anal Chim Acta 822: 1-22.

Ivask A, George S, Bondarenko O, Kahru A. 2012. Metal-containing nano-antimicrobials: differentiating the impact of solubilized metals and particles. In: Nano-antimicrobials - Progress and Prospects. N. Cioffi, Springer**:** 253–290.

Ivask A, Juganson K, Bondarenko O, Mortimer M, Aruoja V, Kasemets K, Blinova I, Heinlaan M, Slaveykova V, Kahru A. 2014. Mechanisms of toxic action of Ag, ZnO and CuO nanoparticles to selected ecotoxicological test organisms and mammalian cells *in vitro*: A comparative review. Nanotoxicology 8(sup1): 57-71.

Ivask A, Titma T, Visnapuu M, Vija H, Kakinen A, Sihtmae M, Pokhrel S, Madler L, Heinlaan M, Kisand V, Shimmo R, Kahru A. 2015. Toxicity of 11 metal oxide nanoparticles to three mammalian cell types *in vitro*. Curr Topics Med Chem 15(18): 1914-1929.

Jiang X, Miclăuş T, Wang L, Foldbjerg R, Sutherland DS, Autrup H, Chen C, Beer C. 2015. Fast intracellular dissolution and persistent cellular uptake of silver nanoparticles in CHO-K1 cells: implication for cytotoxicity. Nanotoxicology 9(2): 181-189.

Karlsson HL, Cronholm P, Gustafsson J, Moller L. 2008. Copper oxide nanoparticles are highly toxic: a comparison between metal oxide nanoparticles and carbon nanotubes. Chem Res Toxicol 21.

Karlsson HL, Gliga AR, Calléja FM, Gonçalves CS, Wallinder IO, Vrieling H, Fadeel B, Hendriks G. 2014. Mechanism-based genotoxicity screening of metal oxide nanoparticles using the ToxTracker panel of reporter cell lines. Part Fibre Toxicol 11(1): 1-14.

Kropf AJ, Chattopadhyay S, Shibata T, Lang EA, Zyryanov VN, Ravel B, McIvor K, Kemner KM, Scheckel KG, Bare SR, Terry J, Kelly SD, Bunker BA, Segre CU. 2010. The new mrcat (Sector 10) bending magnet beamline at theadvanced photon source. AIP Conf Proc 1234, 299

Qu Y, Li W, Zhou Y, Liu X, Zhang L, Wang L, Li Y-f, Iida A, Tang Z, Zhao Y, Chai Z, Chen C. 2011. Full assessment of fate and physiological behavior of quantum dots utilizing *Caenorhabditis elegans* as a model organism. Nano Lett 11(8): 3174-3183.

Ravel B, Newville M. 2005. ATHENA, ARTEMIS, HEPHAESTUS: data analysis for X-ray absorption spectroscopy using IFEFFIT. J Synchr Rad 12: 537–541

Semisch A, Ohle J, Witt B, Hartwig A. 2014. Cytotoxicity and genotoxicity of nano - and microparticulate copper oxide: role of solubility and intracellular bioavailability. Part Fibre Toxicol 11(1): 1-16.

Shi J, Abid AD, Kennedy IM, Hristova KR,Silk WK. 2011. To duckweeds (*Landoltia punctata*), nanoparticulate copper oxide is more inhibitory than the soluble copper in the bulk solution. Environ Pollut 159(5): 1277-1282.

Trzaskowski B, Adamowicz L, Deymier PA. 2008. A theoretical study of zinc(II) interactions with amino acid models and peptide fragments. JBIC J Biol Inorg Chem 13(1): 133-137.

Turney TW, Duriska MB, Jayaratne V, Elbaz A, O'Keefe SJ, Hastings AS, Piva TJ, Wright PFA, Feltis BN. 2012. Formation of Zinc-Containing Nanoparticles from Zn^{2+} Ions in Cell Culture Media: Implications for the Nanotoxicology of ZnO. Chem Res Toxicol 25(10): 2057-2066.

Wang L, Zhang T, Li P, Huang W, Tang J, Wang P, Liu J, Yuan Q, Bai R, Li B, Zhang K, Zhao Y,Chen C. 2015. Use of synchrotron radiation-analytical techniques to reveal chemical origin of silver-nanoparticle cytotoxicity. ACS Nano 9(6): 6532-6547.

Wang P, Menzies NW, Lombi E, McKenna BA, Johannessen B, Glover CJ, Kappen P, Kopittke PM. 2013. Fate of ZnO nanoparticles in soils and cowpea (*Vigna unguiculata*). Environ Sci Technol 47(23): 13822-13830.

Yin H, Casey PS, McCall MJ. 2010. Surface modifications of ZnO nanoparticles and their cytotoxicity. J Nanosci Nanotechnol 10(11): 7565-7570.

Zhang J, He X, Zhang P, Ma Y, Ding Y, Wang Z, Zhang Z. 2015. Quantifying the dissolution of nanomaterials at the nano-bio interface. Sci China Chem 58(5): 761-767.

Zhang P, Ma Y, Zhang Z, He X, Zhang J, Guo Z, Tai R, Zhao Y,Chai Z. 2012. Biotransformation of ceria nanoparticles in cucumber plants. ACS Nano 6(11): 9943-9950.

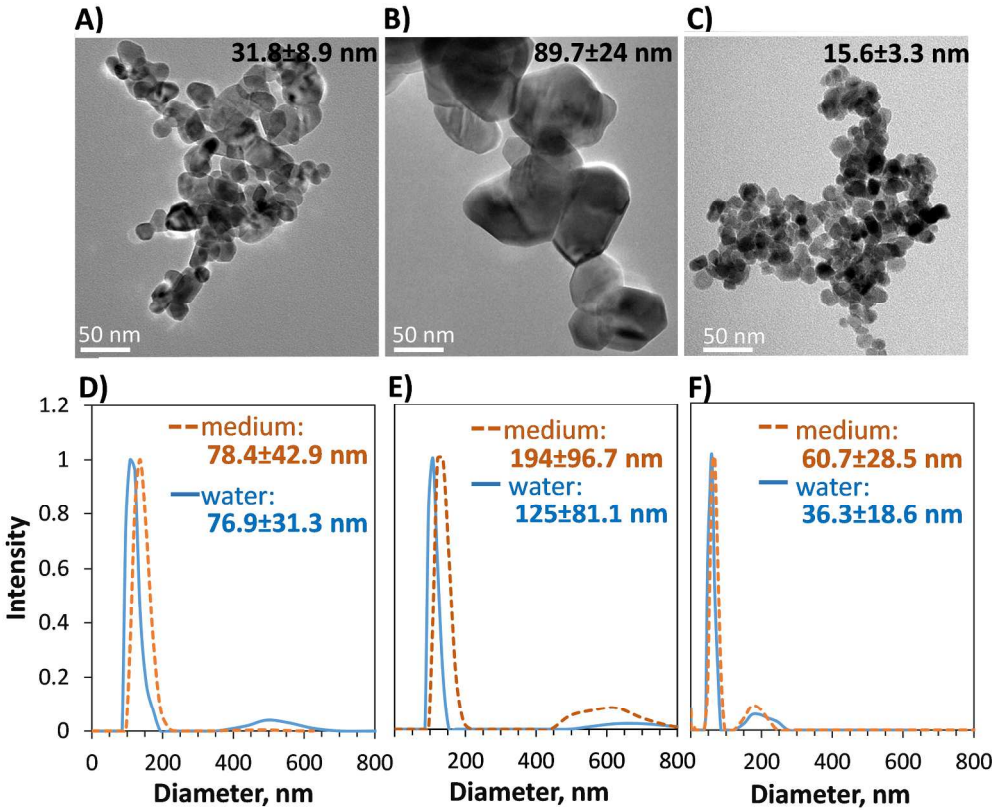

Figure 1

230x186mm (300 x 300 DPI)

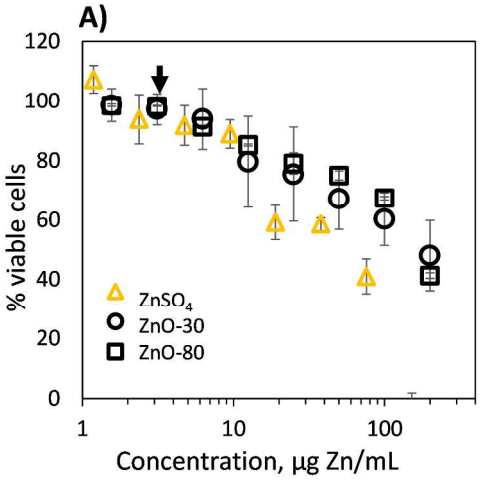

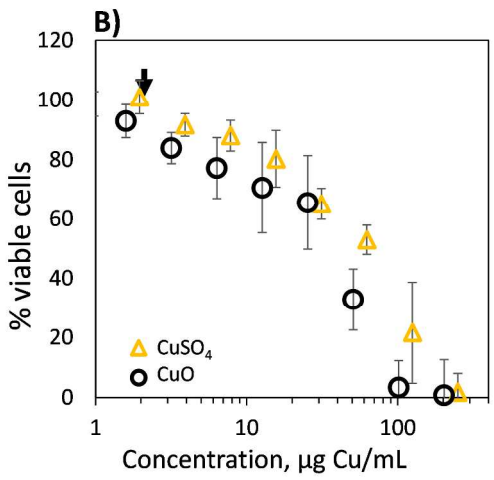

	µg Zn/mL			
	EC_5 (SE)	EC_{10} (SE)	EC_{20} (SE)	EC_{50} (SE)
$ZnSO_4$	4.5 (0.6)	8.9 (0.6)	21.0 (0.8)	96.9 (0.8)
ZnO-30	3.6 (1.8)	10.4 (1.6)	25.3 (1.6)	116 (1.2)
ZnO-80	4.2 (2.6)	11.5 (2.0)	27.1 (1.6)	117 (1.4)

	µg Cu/mL			
	EC_5 (SE)	EC_{10} (SE)	EC_{20} (SE)	EC_{50} (SE)
$CuSO_4$	3.2* (1.2)	7.7* (2.0)	17.3 (1.1)	52.5 (1.1)
CuO	2.2* (1.9)	3.9* (1.7)	8.5 (1.4)	35.8 (1.3)

Figure 2

257x211mm (300 x 300 DPI)

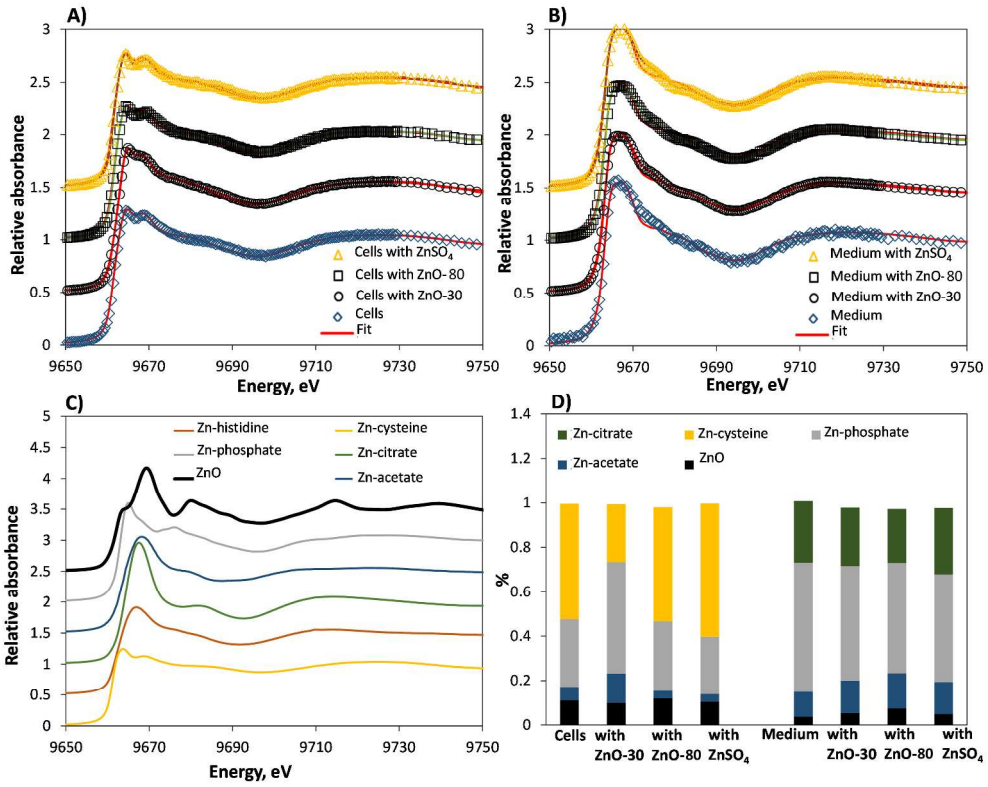

Figure 3

256x200mm (300 x 300 DPI)

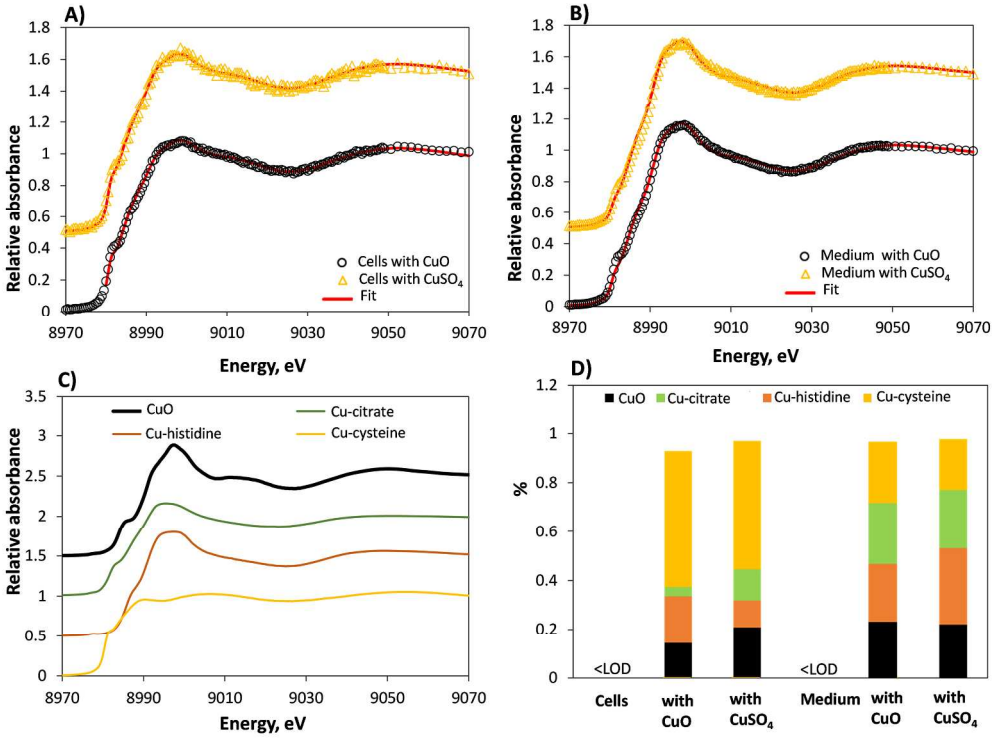

Figure 4

230x170mm (300 x 300 DPI)

Graphical abstract

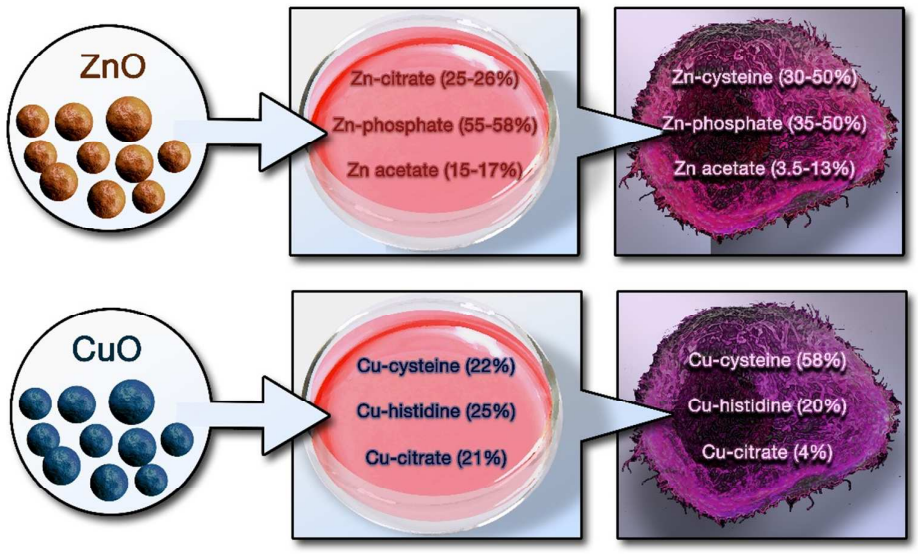

Transformation of ZnO and CuO nanoparticles in cell culture medium and inside the cells